Hindawi Publishing Corporation
International Journal of Engineering Mathematics
Volume 2014, Article ID 905158, 10 pages
http://dx.doi.org/10.1155/2014/905158

Research Article

Influence of Variable Thermal Conductivity on MHD Boundary Layer Slip Flow of Ethylene-Glycol Based Cu Nanofluids over a Stretching Sheet with Convective Boundary Condition

N. Bhaskar Reddy,[1] T. Poornima,[1] and P. Sreenivasulu[2]

[1] *Department of Mathematics, Sri Venkateswara University, Tirupati 517502, India*
[2] *Department of Mathematics, Yogananda Institute of Technology and Science, Tirupati 517520, India*

Correspondence should be addressed to T. Poornima; poonima.anand@gmail.com

Received 24 May 2014; Revised 2 October 2014; Accepted 2 October 2014; Published 6 November 2014

Academic Editor: J. A. Tenreiro Machado

An analysis is carried out to investigate the influence of variable thermal conductivity and partial velocity slip on hydromagnetic two-dimensional boundary layer flow of a nanofluid with Cu nanoparticles over a stretching sheet with convective boundary condition. Using similarity transformation, the governing boundary layer equations along with the appropriate boundary conditions are transformed to a set of ordinary differential equations. Employing Runge-kutta fourth-order method along with shooting technique, the resultant system of equations is solved. The influence of various pertinent parameters such as nanofluid volume fraction parameter, the magnetic parameter, radiation parameter, thermal conductivity parameter, velocity slip parameter, Biot number, and suction or injection parameter on the velocity of the flow field and heat transfer characteristics is computed numerically and illustrated graphically. The present results are compared with the existing results for the case of regular fluid and found an excellent agreement.

1. Introduction

The flow analysis of nanofluids has been the topic of extensive research, due to its enhanced thermal conductivity behavior in heat transfer processes. Nanofluid is a new class of heat transfer fluid (the term nanofluid was coined by Choi [1]) that contains a base fluid and nanosized material particles (diameter less than 100 nm) or fibers suspended in the ordinary fluids. Nanoparticles are made from various materials, such as oxide ceramics (Al_2O_3, CuO), nitride ceramics (AlN, SiN), carbide ceramics (SiC, TiC), metals (Cu, Ag, Au), semiconductors, (TiO_2, SiC), carbon nanotubes, and composite materials such as alloyed nanoparticles or nanoparticle core-polymer shell composites. According to Prodanovi et al. [2], nanofluids containing ultrafine nanoparticle have the capability of flowing in porous media, and these flows can improve oil recovery; hence, nanoparticles are able to control the processes of oil recovery. To improve oil recovery of viscous oils, a fluid, for example, water, is injected into the porous medium to displace the oil, since water viscosity is inferior to that of oil. However, increasing the injected fluid viscosity using nanofluids would drastically increase the recovery efficiency. Nanoparticles can also be used to determine changes in fluid saturation and reservoir properties during oil and gas production.

Many studies on nanofluids are being conducted by scientists and engineers due to their diverse technical and biomedical applications. Examples include nanofluid coolant (electronics cooling, vehicle cooling, and so on), medical applications (cancer therapy and safer surgery by cooling), process industries (materials and chemicals, detergency, food and drink, oil and gas, paper and printing, and textiles), advances in nanoelectronics, nanophotonics, and nanomagnetics; ultrahigh performance cooling is necessary for many industrial technologies.

The nanofluids are more stable and have acceptable viscosity and better wetting, spreading, and dispersion properties on solid surface [3, 4]. The characteristic feature of nanofluids is thermal conductivity enhancement, a phenomenon observed by Masuda et al. [5]. This phenomenon suggests the possibility of using nanofluids in advanced nuclear systems (Buongiorno and Hu [6]). A benchmark study on the thermal conductivity of nanofluids was made by Buongiorno et al. [7]. Das et al. [8] studied a two- to fourfold increase in thermal conductivity enhancement for water-based nanofluids containing Al_2O_3 or CuO nanoparticles over a small temperature range, 21°C–51°C.

The study of boundary layer flow and heat transfer over a stretching surface has attracted considerable attention in many fields of science and technology. Few of these applications, such as wire and fiber coating, materials manufactured polymer extrusion, food stuff processing, drawing of copper wires, and chemical processing equipment. Pioneering work on the dynamics of boundary layer flow over stretching surface was done by Crane [9], who examined the two-dimensional Navier-Stokes equations. Later on, various aspects of the problem have been investigated by Dutta et al. [10], and Chen and Char [11]. Khan and Pop [12] presented the boundary layer flow of nanofluid past a stretching sheet. Recently, Hassani et al. [13] studied an analytical solution for boundary layer flow of a nanofluid past a stretching sheet. Rana and Bhargava [14] analyzed the flow and heat transfer over a nonlinear stretching sheet, a numerical study. Hamad and Ferdows [15] studied the similarity solution of boundary layer stagnation-point flow towards a heated porous stretching sheet saturated with a nanofluid with heat absorption/generation and suction/blowing: a Lie group analysis.

Magnetohydrodynamics (MHD) boundary layer flow over a stretching sheet is important during the last few decades due to its numerous applications in industrial manufacturing processes such as the aerodynamic extrusion of plastic sheets, liquid film, hot rolling, wire drawing, and glass-fiber and paper production. Al-Odat et al. [16] analyzed the thermal boundary layer on an exponentially stretching continuous surface in the presence of magnetic field effect. Chamkha and Aly [17] have presented the MHD free convection flow of a nanofluid past a vertical plate in the presence of heat generation or absorption effects. Later, Aliakbar et al. [18] analyzed the influence of thermal radiation on MHD flow of Maxwellian fluids above stretching sheets. Khan et al. [19] studied the effects of magnetic field on radiative flow of a nanofluid past a stretching sheet. Ibrahim and Shankar [20] analyzed MHD boundary layer flow and heat transfer of a nanofluid past a permeable stretching sheet with slip conditions.

However, radiation heat transfer has a key impact in high temperature regime. Many technological processes occur at high temperature and good working knowledge of radiative heat transfer plays an instrumental role in designing the pertinent equipment. In many practical applications depending on the surfaces properties and solid geometry, the radiative transport is often comparable with that of convective heat transfer. But, unfortunately, little is known about the effects of radiation on the boundary layer flow of a radiating fluid. In fact, a few difficulties arise in studying radiative fluid flow. Firstly, when radiative heat transfer takes place, the radiation is absorbed/emitted not only at system boundaries but also in the interior of the system; hence, prediction of fluid absorption is a difficult task. Secondly, the absorption coefficient of the absorbing emitting fluids is, in general, strongly dependent on wavelength. Thirdly, presence of radiation term in the energy equation makes the equation highly nonlinear. This all leads to computational difficulty. Owing to these difficulties, the effect of radiation on convective flows has been investigated with reasonable simplifications. A good literature on radiative transfer can be seen in well-presented texts by Sparrow and Cess [21] Özisik [22], Siegel and Howell [23], and Howell [24]. Takhar et al. [25] studied radiation effect on the free convection flow of a gas past a semi-infinite plate. Hossain and Takhar [26] investigated mixed convection along a vertical plate with uniform surface temperature taking radiation into account.

The nonadherence of the fluid to a solid boundary, known as velocity slip, is a phenomenon that has been observed under certain circumstances [27]. It is a well-known fact that a viscous fluid normally sticks to the boundary. But, there are many fluids, for example, particulate fluids, rarefied gas etc., where there may be a slip between the fluid and the boundary [28]. The effects of slip conditions are very important in technological applications such as in the polishing of artificial heart valves and the internal cavities [29]. The foremost study taking into account the slip boundary condition over a stretching sheet was conducted by Anderson [30]. A closed form solution of full Navier-Stokes equations for a hydrodynamic flow over a stretching sheet was studied by him. Next to Anderson, Wang [31] solved the full Navier-Stokes' equations with partial slip past a stretching sheet. He continues to investigate stagnation slip flow and heat transfer on a moving plate [32]. Fang et al. [33] analyzed the slip condition of a MHD viscous flow over a stretching sheet. Hayat et al. [34] extended the problem of the previous researchers by incorporating the thermal slip condition and discussed unsteady magneto hydrodynamic flow and heat transfer over a permeable stretching sheet with slip condition also. In a similar way, Abu Bakar et al. [35] studied the boundary layer flow over a stretching sheet with a convective boundary condition and slip effect.

But so far, no attempt has been made to analyze the effects of variable thermal conductivity and velocity slip on MHD boundary layer flow of Ethylene-Glycol based Cu nanofluids over a stretching sheet with convective boundary condition. Thus, the problem is investigated. The surface exhibits convective heating boundary conditions [36–42]. Recently, Alsaedi et al. [43] studied the effects of heat generation/absorption on stagnation point flow of nanofluid over a surface with convective boundary conditions. Masood Khan et al. [44] investigated the MHD Falkner-Skan flow with mixed convection and convective boundary conditions. An efficient numerical shooting technique with a fourth-order Runge-Kutta scheme as used to solve the normalized boundary layer equations and the effects of material parameters on the flow field and heat transfer characteristics is discussed in detail.

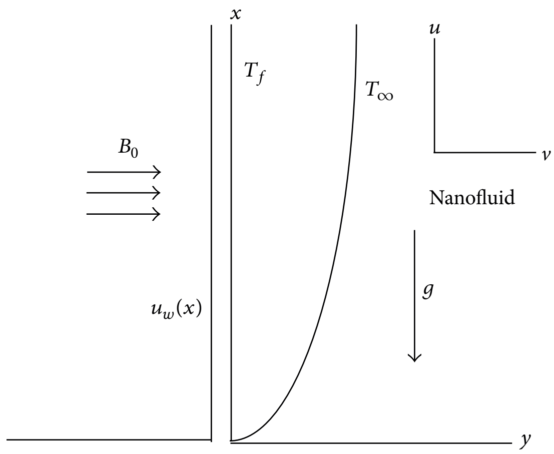

Figure 1: Physical model of the system.

2. Mathematical Analysis

A two-dimensional steady laminar boundary layer flow of a viscous incompressible flow of nanofluid past a permeable stretching sheet coinciding with the plane $y = 0$ is considered. The flow is confirmed to $y > 0$. The fluid is assumed to be gray, absorbing-emitting radiation but nonscattering medium. The flow is generated due to stretching of the sheet, caused by the simultaneous application of two equal and opposite forces along the x-axis. Keeping the origin fixed, the sheet is then stretched with velocity $u_w(x) = ax$, where a is constant. A uniform magnetic field is applied in the direction transverse to the stretching surface. The transverse applied magnetic field and magnetic Reynolds number are assumed to be very small, so that the induced magnetic field is negligible. There is a constant suction/injection velocity V_w normal to the sheet. The temperature of sheet surface (to be determined later) is the result of a convective heating process which is characterized by a temperature T_f and a heat transfer coefficient h_f. It is to be mentioned that the hole size (in nanoscale) of porous sheet is taken to be constant. The fluid is ethylene-glycol based nanofluid containing copper (Cu). The nanofluid is assumed incompressible and flow is assumed to be laminar. A schematic representation of the physical model and coordinate system is depicted in Figure 1. Under the usual assumptions, the governing boundary layer equations are given by

$$\frac{\partial u}{\partial x} + \frac{\partial v}{\partial y} = 0 \tag{1}$$

$$u\frac{\partial u}{\partial x} + v\frac{\partial u}{\partial y} = \frac{1}{\rho_{nf}}\left[\mu_{nf}\frac{\partial^2 u}{\partial y^2} + g(\rho\beta)_{nf}(T - T_\infty) - \sigma B_0^2 u\right] \tag{2}$$

$$u\frac{\partial T}{\partial x} + v\frac{\partial T}{\partial y} = \frac{1}{(\rho C_p)_{nf}}\frac{\partial}{\partial y}\left(k_{nf}^*\frac{\partial T}{\partial y} - q_r\right). \tag{3}$$

The boundary conditions for the velocity and temperature fields are

$$u = u_w + A\frac{\partial u}{\partial y}, \qquad v = -v_w, \qquad -k_f\frac{\partial T}{\partial y} = h_f\left(T_f - T_\infty\right) \quad \text{at } y = 0$$
$$u \longrightarrow 0, \quad T \longrightarrow T_\infty \quad \text{as } y \longrightarrow \infty, \tag{4}$$

where u and v are the velocity components in the x and y directions, respectively, T is the temperature of the nanofluid, T_∞ is the ambient fluid temperature, g is the acceleration due to gravity, σ is the electric conductivity, B_0 is the uniform magnetic field strength, and q_r is the radiative heat flux. A is the velocity slip factor. v_w is the wall mass flux with $v_w < 0$ for suction and $v_w > 0$ for injection, respectively. k_f is the thermal conductivity of the ordinary fluid and T_f is the temperature of the hot fluid.

It should be mentioned that such slip conditions were recently used in a series of papers [45–50]. It is worth mentioning at this end that fluid flow with slip is important in microelectromechanical systems (MEMS). The flow in these systems deviates significantly from the traditional no slip flow because of the microscale dimensions of these devices. MEMS barometers and commercially compatible flexible printed circuit boards are examples for stretchable MEMS [51].

The variable thermal conductivity (Arunachalam and Rajappa [52], Chiam [53] and Seddeek and Salem [54]) is considered to vary linearly with temperature as given below

$$k^* = k\left[1 + \epsilon\,\theta\right], \tag{5}$$

where k is thermal conductivity parameter.

The effective density of the nanofluid is given by

$$\rho_{nf} = (1 - \phi)\,\rho_f + \phi\rho_s, \tag{6}$$

where ϕ is the solid volume fraction of nanoparticles. Thermal diffusivity of nanofluid is

$$\alpha_{nf} = \frac{k_{nf}}{(\rho C_p)_{nf}}, \tag{7}$$

where the heat capacitance C_p of the nanofluid is obtained as

$$(\rho C_p)_{nf} = (1 - \phi)(\rho C_p)_f + \phi(\rho C_p)_s. \tag{8}$$

The thermal conductivity of the nanofluid k_{nf} for spherical nanoparticles can be written as (Maxwell [55])

$$\frac{k_{nf}}{k_f} = \frac{(k_s + 2k_f) - 2\phi(k_f - k_s)}{(k_s + 2k_f) + \phi(k_f - k_s)}. \tag{9}$$

The thermal expansion coefficient of the nanofluid can be determined by

$$(\rho\beta)_{nf} = (1 - \phi)(\rho\beta)_f + \phi(\rho\beta)_s. \tag{10}$$

Table 1: Thermophysical properties of fluid and nanoparticles [55, 56].

Physical properties	Fluid phase (ethylene-glycol)	Cu
Cp (J/kg K)	1114.4	385
ρ (kg/m^3)	2415	8933
$\beta \times 10^{-5}$ (1/K)	65	1.67
k (W/m K)	0.252	401

Also the effective dynamic viscosity of the nanofluid given by Brinkman [56] can be written as

$$\mu_{nf} = \frac{\mu_f}{(1-\phi)^{2.5}}. \tag{11}$$

Here the subscripts nf, f, and s represent the thermophysical properties of the nanofluids, base fluid, and nanosolid particles, respectively (Table 1).

By using the Rosseland diffusion approximation (Prasad et al. [57]), the radiative heat flux is given by

$$q_r = -\frac{4}{3}\frac{\sigma^*}{k^*}\frac{\partial T^4}{\partial y}, \tag{12}$$

where σ^* is the Stefan-Boltzmann constant and k^* is the mean absorption coefficient. It should be noted that, by using the Rosseland approximation, the present analysis is limited to optically thick fluids. Taking the refractive index of the gas medium to be constant, unidirectional radiation flux q_r is considered and it is assumed that $\partial q_r/\partial y \gg \partial q_r/\partial x$. This model is valid for optically thick media in which thermal radiation propagates only a limited distance prior to experiencing scattering or absorption. The local thermal radiation intensity is due to radiation emitting from proximate locations in the vicinity of which emission and scattering are comparable to the location of interest. The energy transfer depends on conditions only in the area adjacent to the plate regime, that is, the boundary layer regime. Rosseland's model yields accurate results for intensive absorption, that is, optically thick flows which are optically far from the boundary surface. Implicit in this approximation is also the existence of wavelength regions where the optical thickness may exceed a value of five. As such, the Rosseland model, while limited compared with other flux models, can simulate to a reasonable degree of accuracy thermal radiation in problems ranging from thermal radiation transport via gases at low density to thermal radiation simulations associated with nuclear blast waves. If the temperature differences within the flow are sufficiently small, then (12) can be linearized by expanding T^4 into the Taylor series about T_∞, which after neglecting higher-order terms takes the form

$$T^4 \cong 4T_\infty^3 T - 3T_\infty^4. \tag{13}$$

In view of (12) and (13), (3) becomes

$$u\frac{\partial T}{\partial x} + v\frac{\partial T}{\partial y} = \alpha_{nf}\left[\left(1 + \epsilon\,\theta + \frac{4}{3}\mathrm{Nr}\right)\frac{\partial^2 T}{\partial y^2} + \frac{\epsilon}{\left(T_f - T_\infty\right)}\left(\frac{\partial T}{\partial y}\right)^2\right], \tag{14}$$

where $\mathrm{Nr} = 16\sigma^* T_\infty^3 / 3k_{nf}k^*$ is the radiation parameter.

To get similarity solutions of (1)–(3) subject to the boundary conditions (4), we introduce the following similarity transformations:

$$\eta = \left(\frac{a}{\nu_f}\right)^{1/2} y, \qquad u = axf'(\eta), \qquad v = -\left(a\nu_f\right)^{1/2},$$
$$\theta = \frac{T - T_\infty}{T_f - T_\infty}, \qquad M = \frac{\sigma B_0^2}{a\rho_f},$$
$$\lambda = \frac{g(\rho\beta)_f\left(T_f - T_\infty\right)}{\rho_f a u_w}, \qquad \mathrm{Nr} = \frac{4\sigma^* T_\infty^3}{k^* k_{nf}},$$
$$\mathrm{Pr} = \frac{\nu_f}{\alpha_f}, \qquad S = -\frac{v_w}{\sqrt{a\nu_f}},$$
$$\delta = A\sqrt{\frac{a}{\nu_f}}, \qquad \Gamma = \frac{h_f}{k_f}\sqrt{\frac{\nu_f}{a}}, \tag{15}$$

where ν_f is the kinematic viscosity of the base fluid.

In view of (15), (1), (2), and (14) take the following dimensionless form:

$$f'''(1-\phi)^{2.5}\left[\left(1 - \phi + \phi\frac{\rho_s}{\rho_f}\right)\left(ff'' - f'^2\right) + \left(1 - \phi + \phi\frac{(\rho\beta)_s}{(\rho\beta)_f}\right)\lambda\theta - Mf'\right] = 0$$
$$\left(1 + \frac{4}{3}\mathrm{Nr}\right)\theta'' + \epsilon\,\theta\theta'' + \epsilon\,\theta'^2 + \mathrm{Pr}\left(\frac{k_f}{k_{nf}}\right)\left(1 - \phi + \phi\frac{\left(\rho C_p\right)_s}{\left(\rho C_p\right)_f}\right) f\theta' = 0, \tag{16}$$

where prime denotes the differentiation with respect to η.

The corresponding boundary conditions are

$$f'(0) = 1 + \delta f''(0), \qquad f(0) = S,$$
$$\theta'(0) = -\Gamma(1 - \theta(0)) \tag{17}$$
$$f'(\infty) \longrightarrow 0, \quad \theta(\infty) \longrightarrow 0.$$

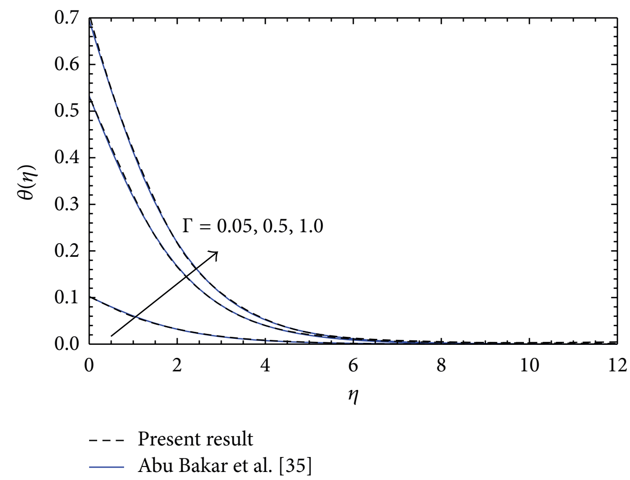

FIGURE 2: Comparison of temperature profiles for different Γ.

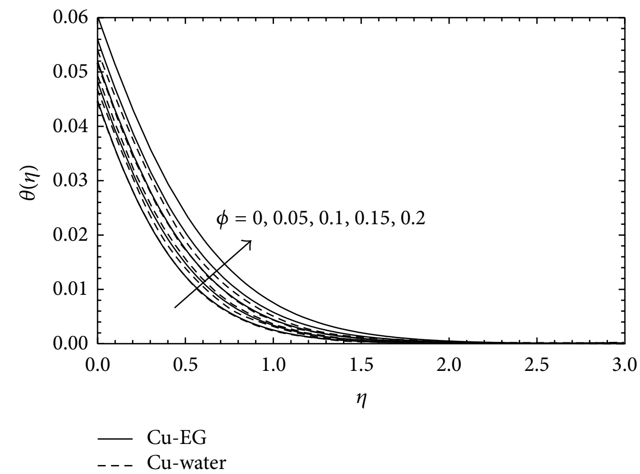

FIGURE 3: Temperature profiles for different values of ϕ.

The quantities of practical interest in this study are the skin friction or the shear stress coefficient C_f and the local Nusselt number Nu_x, which are defined as

$$C_f = -\frac{\mu_{nf}}{\rho_f u_w^2}\left(\frac{\partial u}{\partial y}\right)_{y=0}$$
$$\mathrm{Nu}_x = \frac{x k_{nf}}{k_f\left(T_w - T_\infty\right)}\left(-\frac{\partial T}{\partial y}\right)_{y=0}. \tag{18}$$

Using (6), the skin friction coefficient and local Nusselt number can be expressed as

$$\mathrm{Re}_x^{1/2} C_f = -\frac{1}{(1-\phi)^{2.5}} f''(0)$$
$$\mathrm{Re}_x^{1/2}\mathrm{Nu}_x = -\frac{k_{nf}}{k_f}\theta'(0), \tag{19}$$

where $\mathrm{Re}_x = u_w x/\nu_f$ is the Reynolds number.

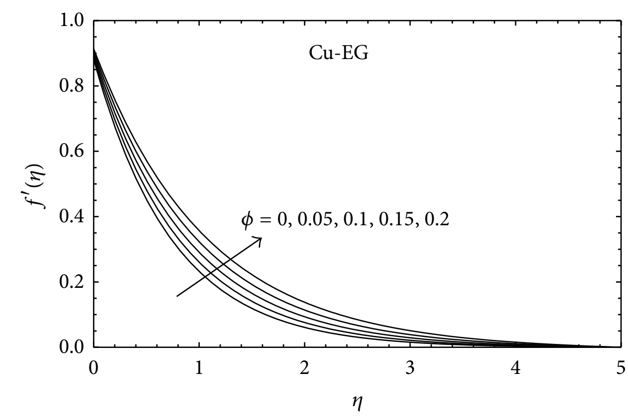

FIGURE 4: Velocity profiles for different values of ϕ.

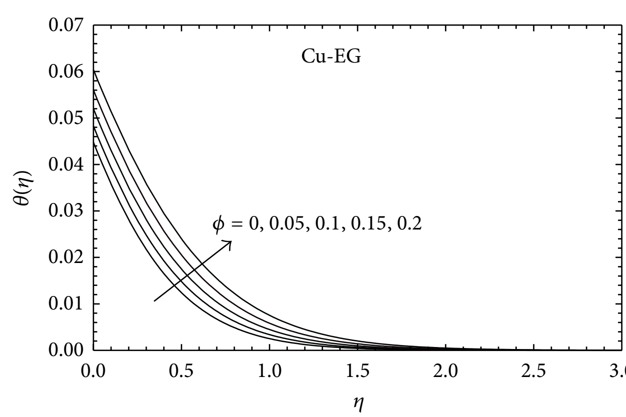

FIGURE 5: Temperature profiles for different values of ϕ.

3. Results and Discussion

The coupled nonlinear differential equations (16) along with the boundary conditions (17) are solved numerically using Runge-Kutta fourth order technique along with shooting method. The integration length η_∞ varies with the parameter values and it has been suitably chosen each time such that the boundary conditions at the outer edge of the boundary layer are satisfied. In order to bring out the salient features of the flow and the heat transfer characteristics in the Cu-EG based nanofluid, the numerical values for different values of the governing parameters ϕ, M, ϵ, Nr, δ, S, and Γ are computed and portrayed in Figures 2–13.

In order to validate our analysis, the present results are compared with the existing results for the case of regular fluid and found an excellent agreement (Figure 2).

Figure 3 shows the temperature profiles for different values of the nanoparticle volume fraction ϕ with water and EG based nanofluids. It is found that the temperature increases with an increase in the nanoparticle volume fraction for both Cu-water and Cu-EG based fluid. And also it is noticed that EG based nanofluids have more impact in rising the temperature than that of water-based nanofluids. This is due to the fact that the thermal conductivity increases and

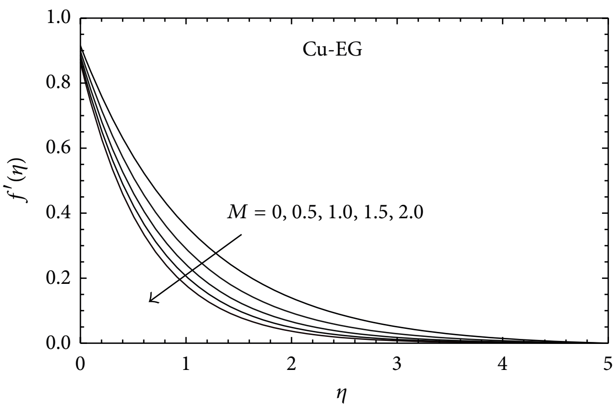

Figure 6: Velocity profiles for different values of M.

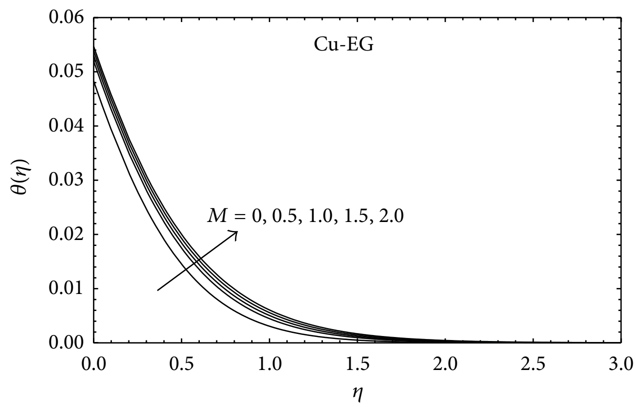

Figure 7: Temperature profiles for different values of M.

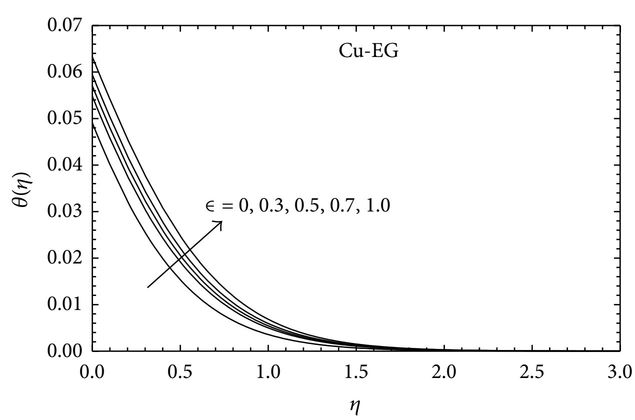

Figure 8: Temperature profiles for different values of ϵ.

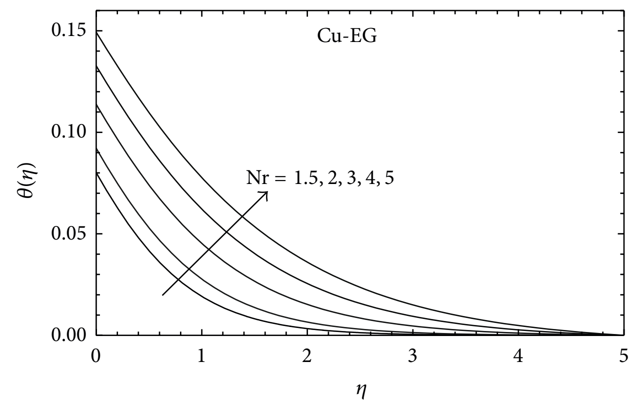

Figure 9: Temperature profiles for different values of Nr.

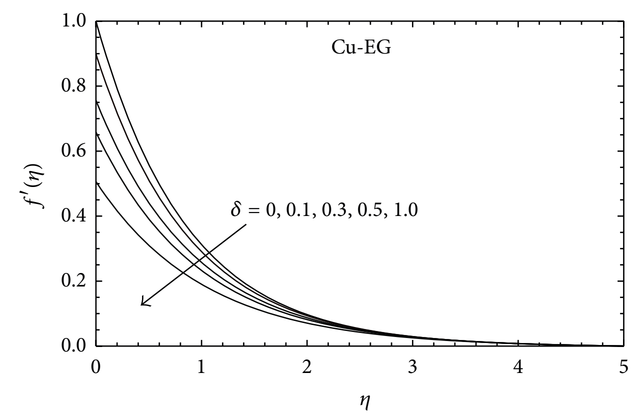

Figure 10: Velocity profiles for different values of δ.

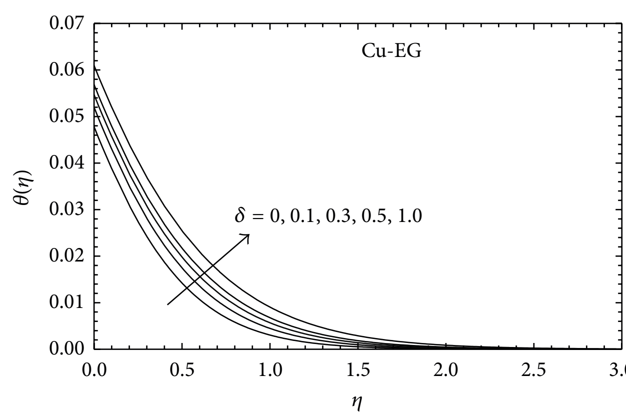

Figure 11: Temperature profiles for different values of δ.

then the thermal boundary layer thickness increases with the increase in volume of nanoparticles. Also it is observed that the thermal conductivity is more in ethylene-glycol based nanofluid when compared to water-based nanofluid.

Figures 4 and 5 represent the influence of the nanoparticle volume fraction on the velocity and temperature. It is found that both the nanofluid velocity and the temperature increase with an increase in nanoparticle volume fraction. These figures illustrate in agreement with the physical behavior that the thermal conductivity increases and then the thermal boundary layer thickness increases with the increase in volume of nanoparticles.

Effect of the magnetic parameter M on the velocity and temperature profiles is shown in Figures 6 and 7, respectively. It is observed that the velocity decreases as the magnetic parameter increases (Figure 6). The presence of magnetic field, normal to the flow in an electrically conducting fluid, gives rise to a resistive type of force called Lorentz force,

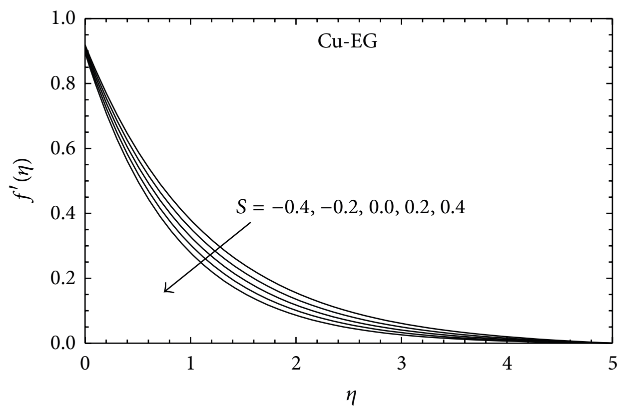

Figure 12: Velocity profiles for different values of S.

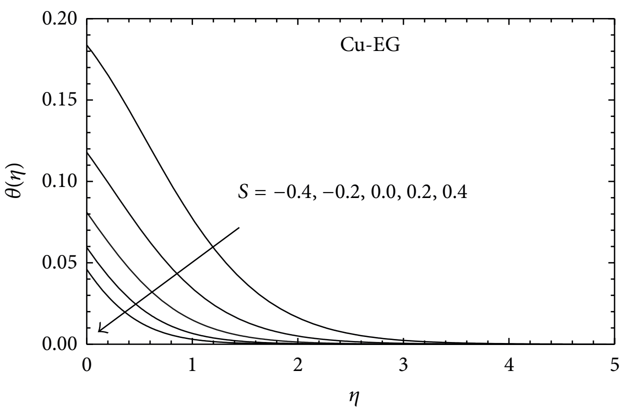

Figure 13: Temperature profiles for different values of S.

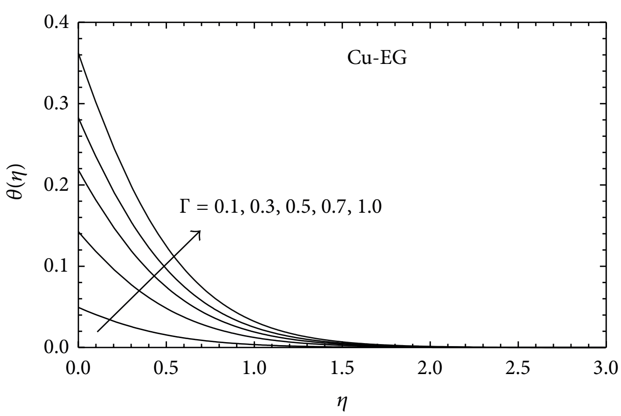

Figure 14: Temperature profiles for different values of Γ.

which retards the fluid flow. This resistive force controls the nanofluids velocity which is useful in numerous applications such as magnetohydrodynamic power generation and electromagnetic coating of wires and metal. Since the magnetic parameter is inversely proportional to density, so, for ascending M, ρ descends, thus increasing the temperature of the fluid (Figure 7).

Figure 8 illustrates the temperature profiles for various values of thermal conductivity parameter ϵ. It is clear from our definition that $k^* > k$; that is, the thermal conductivity is higher when $\epsilon > 0$ and hence an increase in ϵ results in increase of thermal conductivity, thereby raising the temperature.

The influence of effect of radiation parameter Nr on temperature is portrayed in Figure 9. The effect of Nr is prominently seen throughout the boundary layer. It is interesting to observe that the effect of Nr is to increase the temperature distribution. The radiation parameter (reciprocal of Stephan number) is the measure of relative importance of thermal radiation transfer to the conduction heat transfer. Thus larger values of N sound dominance of thermal radiation over conduction. Consequently larger values of N are indicative of larger amount of radiative heat energy being poured into the system, causing rise in $\theta(\eta)$.

Figures 10 and 11 demonstrate the variation of the streamwise velocity and temperature for different values of slip parameter δ. As the slip parameter increases, the slip at the surface wall increases and a smaller amount of penetration occurs due to the stretching surface into the fluid. In the no slip condition, δ approaches zero; then $f'(0) = 1$. It is clear from the figures that the velocity component at the wall reduces with an increase in the slip parameter δ and decreases asymptotically to zero at the edge of the hydrodynamic boundary layer. Thus hydrodynamic boundary layer thickness decreases as the slip parameter δ increases for both the regular and nanofluids and, as a result, the local velocity also decreases. This is in agreement with the fact that higher δ implies an increase in the lubrication and slipperiness of the surface. On the other hand, it is evident from Figure 11 that the surface slipperiness affects the temperature of the fluid inversely; that is, an increase with slip parameter tends to increase temperature of the fluid. By escalating δ, thermal boundary layer thickness enhances. So, we can interpret that the rate of heat transfer decreases with the increase in slip parameter δ.

The effect of suction or injection parameter S on the velocity and temperature is shown in Figures 12 and 13, respectively. It is observed that the velocity decreases with increase in the suction/injection parameter. The physical explanation for such behavior is as follows: in case of suction, the heated fluid is pushed towards the wall where the buoyancy forces can act to retard the fluid due to high influence of the viscosity (Figure 12). The thermal boundary layer thickness for the injection is more pronounced than for suction and it is quite superior for Cu-EG than for pure water (regular fluid, $\phi = 0$). Figure 13 explains that, for both suction/injection, the existence of Cu nanoparticle increases the thermal conductivity rapidly, which leads to an increase in the thickness of the thermal boundary layer. Thus the temperature of the fluid rises.

Figure 14 depicts the temperature profiles for different values of convective parameter Γ. It is clearly seen that the increases in the convective parameter increase the temperature profile and thereby reduce the thermal boundary layer thickness. The variations of $-f''(0)$ and $-\theta'(0)$ which are proportional to the local skin-friction coefficient and rate of heat transfers are shown in Tables 2–7. From Table 2, it is found that both the wall skin friction coefficient and heat transfer

Table 2: Values of $-f''(0)$ and $-\theta'(0)$ for various values of ϕ.

ϕ	$-f''(0)$	$-\theta'(0)$
0.0	1.177071	0.0955225
0.05	1.093940	0.0951172
0.10	1.013062	0.0947067
0.15	0.934425	0.0942881
0.2	0.858128	0.0938579

Table 3: Values of $-f''(0)$ and $-\theta'(0)$ for various values of ϕ and ϵ.

ϕ	ϵ	$-f''(0)$	$-\theta'(0)$
0.0	0.0	1.17702	0.0955518
	0.3	1.17691	0.0952439
	0.5	1.17684	0.0950191
	0.7	1.17675	0.0947772
	1.0	1.1766	0.0943792
0.1	0.0	1.01307	0.0945435
	0.3	1.01298	0.0942011
	0.5	1.01292	0.0939533
	0.7	1.01285	0.0936886
	1.0	1.01273	0.0932570

Table 4: Values of $-f''(0)$ and $-\theta'(0)$ for various values of ϕ and Nr.

ϕ	Nr	$-f''(0)$	$-\theta'(0)$
0.0	1.5	1.17585	0.0931194
	2.0	1.17523	0.0920499
	3.0	1.17396	0.0900892
	4.0	1.17269	0.0883290
	5.0	1.17147	0.0867510
0.1	1.0	1.01157	0.0921196
	2.0	1.01090	0.0909412
	3.0	1.00953	0.0888097
	4.0	1.00821	0.0869363
	5.0	1.00698	0.0852933

rate at the surface decrease as ϕ increases. From Table 3, it is observed that the skin friction coefficient at the wall decreases with an increase in the parameter ϵ for both regular fluid and nanofluid. Also it is seen that the rate of heat transfer decreases with an increase in the value of ϵ. This happens due to the fact that with the increase in ε the thermal conductivity increases which lowers the temperature gradient at the plate surface. From Table 4, it is clear that both the skin friction and heat transfer rate decrease with an increase in the radiation parameter Nr.

Table 5 shows the effects of wall skin friction and rate of heat transfer with suction/injection parameter S for regular fluid and nanofluid. It is evident that increasing suction ($S > 0$) at the wall tends to have high heat transfer rate but injection ($S < 0$) decreases heat transfer rate. It is also noted that the addition of nanoparticle produces a remarkable enhancement on heat transfer with respect to that of pure fluid.

Table 5: Values of $-f''(0)$ and $-\theta'(0)$ for various values of ϕ and S.

ϕ	S	$-f''(0)$	$-\theta'(0)$
0.0	0.3	1.17701	0.0955225
	0.2	1.13491	0.0948018
	0.1	1.09395	0.0938647
	0.0	1.05412	0.092619
	−0.1	1.01538	0.0909242
	−0.2	0.97764	0.0885645
	−0.3	0.940748	0.0852126
0.1	0.3	1.26325	0.0945107
	0.2	1.20846	0.0936994
	0.1	1.1555	0.0926697
	0.0	1.10444	0.0913403
	−0.1	1.05532	0.0895938
	−0.2	1.00811	0.0872611
	−0.3	0.962756	0.0841031

Table 6: Values of $-f''(0)$ and $-\theta'(0)$ for various values of ϕ and δ.

ϕ	δ	$-f''(0)$	$-\theta'(0)$
0.0	0.0	1.38291	0.0956796
	0.3	0.917088	0.0952758
	0.5	0.756782	0.0950839
	0.7	0.646713	0.0949264
	1.0	0.532992	0.0947331
0.1	0.0	1.51052	0.0947236
	0.3	0.96444	0.0941837
	0.5	0.786612	0.0939336
	0.7	0.66708	0.0937302
	1.0	0.545629	0.0934822

Table 7: Values of $-f''(0)$ and $-\theta'(0)$ for various values of ϕ and Γ.

ϕ	Γ	$-f''(0)$	$-\theta'(0)$
0.0	0.1	1.17701	0.0955225
	0.3	1.17516	0.262626
	0.5	1.17355	0.403359
	0.7	1.17215	0.523035
	1.0	1.17036	0.67177
0.1	0.1	1.26325	0.0945107
	0.3	1.26147	0.255081
	0.5	1.25999	0.385787
	0.7	1.25873	0.493837
	1.0	1.25719	0.624363

From Table 6, we notice that the skin friction coefficient at the wall decreases with an increase in the slip parameter δ for both regular fluid and nanofluid. This is less pronounced with an increase in the value of δ. That is, as expected, for the fluid flows at nanoscales, the shear stress at the wall decreases with an increase in the slip parameter δ. It is noticed that, in the no slip condition problem, the highest wall shear stress occurs. Table 7 shows the effects of surface skin friction and rate of heat transfer with parameter Γ for regular fluid and nanofluid. It is evident that the surface skin friction decreases but the heat transfer rate decreases with an increase in convection parameter Γ.

Conflict of Interests

The authors declare that there is no conflict of interests regarding the publication of this paper.

Acknowledgments

This work is carried out by the financial support of University Grants Commission under Major Research Project (UGC-F. no. 41-794/2012(SR)), for which the first author is highly grateful. The authors are highly grateful to the reviewers for their constructive comments, which helped to enrich the quality of the paper.

References

[1] S. Choi, "Enhancing thermal conductivity of fluids with nanoparticle," in *Developments and Applications of Non-Newtonian Flows*, D. A. Siginer and P. H. Wang, Eds., vol. 66, pp. 99–105, ASME, New York, NY, USA, 1995.

[2] M. Prodanovi, S. Ryoo, and R. A. Rahmani, "Effects of magnetic field on the motion of multiphase fluids containing paramagnetic nanoparticles in porous media," in *Proceedings of the SPE Improved Oil Recovery Symposium*, Tulsa, Okla, USA, 2010.

[3] C. T. Nguyen, G. Roy, C. Gauthier, and N. Galanis, "Heat transfer enhancement using Al_2O_3-water nanofluid for an electronic liquid cooling system," *Applied Thermal Engineering*, vol. 27, no. 8-9, pp. 1501–1506, 2007.

[4] A. Akbarinia, M. Abdolzadeh, and R. Laur, "Critical investigation of heat transfer enhancement using nanofluids in microchannels with slip and non-slip flow regimes," *Applied Thermal Engineering*, vol. 31, no. 4, pp. 556–565, 2011.

[5] H. Masuda, A. Ebata, K. Teramae, and N. Hishinuma, "Alteration of thermal conductivity and viscosity of liquid by dispersing ultra-fine particles," *Netsu Bussei*, vol. 7, pp. 227–233, 1993.

[6] J. Buongiorno and W. Hu, "Nanofluid coolants for advanced nuclear power plants," in *Proceedings of the ICAPP*, Paper no. 5705, Seoul, Republic of Korea, May 2005.

[7] J. Buongiorno, D. C. Venerus, N. Prabhat et al., "A benchmark study on the thermal conductivity of nanofluids," *Journal Applied Physics*, vol. 106, no. 9, Article ID 094312, 2009.

[8] S. K. Das, N. Putra, P. Thiesen, and W. Roetzel, "Temperature dependence of thermal conductivity enhancement for nanofluids," *Journal of Heat Transfer*, vol. 125, no. 4, pp. 567–574, 2003.

[9] L. J. Crane, "Flow past a stretching plate," *Zeitschrift für angewandte Mathematik und Physik*, vol. 21, no. 4, pp. 645–647, 1970.

[10] B. K. Dutta, P. Roy, and A. S. Gupta, "Temperature field in flow over a stretching sheet with uniform heat flux," *International Communications in Heat and Mass Transfer*, vol. 12, no. 1, pp. 89–94, 1985.

[11] C. K. Chen and M. I. Char, "Heat transfer of a continuous, stretching surface with suction or blowing," *Journal of Mathematical Analysis and Applications*, vol. 135, no. 2, pp. 568–580, 1988.

[12] W. A. Khan and I. Pop, "Boundary-layer flow of a nanofluid past a stretching sheet," *International Journal of Heat and Mass Transfer*, vol. 53, no. 11-12, pp. 2477–2483, 2010.

[13] M. Hassani, M. M. Tabar, H. Nemati, G. Domairry, and F. Noori, "An analytical solution for boundary layer flow of a nanofluid past a stretching sheet," *International Journal of Thermal Sciences*, vol. 50, no. 11, pp. 2256–2263, 2011.

[14] P. Rana and R. Bhargava, "Flow and heat transfer of a nanofluid over a nonlinearly stretching sheet: a numerical study," *Communications in Nonlinear Science and Numerical Simulation*, vol. 17, no. 1, pp. 212–226, 2012.

[15] M. A. Hamad and M. Ferdows, "Similarity solution of boundary layer stagnation-point flow towards a heated porous stretching sheet saturated with a nanofluid with heat absorption/generation and suction/blowing: a Lie group analysis," *Communications in Nonlinear Science and Numerical Simulation*, vol. 17, no. 1, pp. 132–140, 2012.

[16] M. Q. Al-Odat, R. A. Damesh, and T. A. Al-Azab, "Thermal boundary layer on an exponentially stretching continuous surface in the presence of magnetic field effect," *International Journal of Applied Mechanics and Engineering*, vol. 11, no. 2, pp. 289–299, 2006.

[17] A. J. Chamkha and A. M. Aly, "MHD free convection flow of a nanofluid past a vertical plate in the presence of heat generation or absorption effects," *Chemical Engineering Communications*, vol. 198, no. 3, pp. 425–441, 2011.

[18] V. Aliakbar, A. Alizadeh-Pahlavan, and K. Sadeghy, "The influence of thermal radiation on MHD flow of Maxwellian fluids above stretching sheets," *Communications in Nonlinear Science and Numerical Simulation*, vol. 14, no. 3, pp. 779–794, 2009.

[19] M. S. Khan, M. M. Alam, and M. Ferdows, "Effects of magnetic field on radiative flow of a nanofluid past a stretching sheet," *Procedia Engineering*, vol. 56, pp. 316–322, 2013.

[20] W. Ibrahim and B. Shankar, "MHD boundary layer flow and heat transfer of a nanofluid past a permeable stretching sheet with velocity, thermal and solutal slip boundary conditions," *Computers & Fluids*, vol. 75, pp. 1–10, 2013.

[21] M. E. Sparrow and D. R. Cess, *Radiation Heat Transfer*, Brooks/Cole, Belmont, Calif, USA, 1970.

[22] N. M. Özisik, *Radiative Transfer and Interaction with Conduction and Convection*, John Wiley & Sons, New York, NY, USA, 1973.

[23] R. Siegel and J. R. Howell, *Thermal Radiation Heat Transfer*, Hemisphere, New York, NY, USA, 2nd edition, 1992.

[24] J. R. Howell, "Radiative transfer in porous media," in *Handbook of Porous Media*, K. Vafai, Ed., pp. 663–698, CRC Press, New York, NY, USA, 2000.

[25] H. S. Takhar, R. S. R. Gorla, and V. M. Soundalgekar, "Radiation effects on MHD free convection flow of a gas past a semi-infinite vertical plate," *International Journal of Numerical Methods for Heat and Fluid Flow*, vol. 6, no. 2, pp. 77–83, 1996.

[26] M. A. Hossain and H. S. Takhar, "Radiation effect on mixed convection along a vertical plate with uniform surface temperature," *Heat and Mass Transfer*, vol. 31, no. 4, pp. 243–248, 1996.

[27] A. Yoshimura and R. K. Prud'homme, "Wall slip corrections for Couette and parallel disk viscometers," *Journal of Rheology*, vol. 32, no. 1, pp. 53–67, 1988.

[28] V. P. Shidlovskiy, *Introduction to the Dynamics of Rarefied Gases*, American Elsevier Publishing, New York, NY, USA, 1967.

[29] S. Mansur and A. Ishak, "The magnetohydrodynamic boundary layer flow of a nanofluid past a stretching/shrinking sheet with

slip boundary conditions," *Journal of Applied Mathematics*, vol. 2014, Article ID 907152, 7 pages, 2014.

[30] H. I. Andersson, "Slip flow past a stretching surface," *Acta Mechanica*, vol. 158, no. 1-2, pp. 121–125, 2002.

[31] C. Y. Wang, "Flow due to a stretching boundary with partial slip—an exact solution of the Navier-Stokes equations," *Chemical Engineering Science*, vol. 57, no. 17, pp. 3745–3747, 2002.

[32] C. Y. Wang, "Stagnation slip flow and heat transfer on a moving plate," *Chemical Engineering Science*, vol. 61, no. 23, pp. 7668–7672, 2006.

[33] T. Fang, J. Zhang, and S. Yao, "Slip MHD viscous flow over a stretching sheet—an exact solution," *Communications in Nonlinear Science and Numerical Simulation*, vol. 14, no. 11, pp. 3731–3737, 2009.

[34] T. Hayat, M. Qasim, and S. Mesloub, "MHD flow and heat transfer over permeable stretching sheet with slip conditions," *International Journal for Numerical Methods in Fluids*, vol. 66, no. 8, pp. 963–975, 2011.

[35] A. Abu Bakar, M. K. A. W. Wan Zaimi, R. Hamid A, B. Bidin, and A. Ishak, "Boundary layer flow over a stretching sheet with a convective boundary condition and slip effect," *World Applied Sciences Journal*, vol. 17, pp. 49–53, 2012.

[36] O. D. Makinde and A. Aziz, "Boundary layer flow of a nanofluid past a stretching sheet with a convective boundary condition," *International Journal of Thermal Sciences*, vol. 50, no. 7, pp. 1326–1332, 2011.

[37] O. D. Makinde and A. Aziz, "MHD mixed convection from a vertical plate embedded in a porous medium with a convective boundary condition," *International Journal of Thermal Sciences*, vol. 49, no. 9, pp. 1813–1820, 2010.

[38] O. D. Makinde, "Similarity solution of hydromagnetic heat and mass transfer over a vertical plate with a convective surface boundary condition," *International Journal of Physical Sciences*, vol. 5, no. 6, pp. 700–710, 2010.

[39] O. D. Makinde, "On MHD heat and mass transfer over a moving vertical plate with a convective surface boundary condition," *Canadian Journal of Chemical Engineering*, vol. 88, no. 6, pp. 983–990, 2010.

[40] S. V. Subhashini, N. Samuel, and I. Pop, "Double-diffusive convection from a permeable vertical surface under convective boundary condition," *International Communications in Heat and Mass Transfer*, vol. 38, no. 9, pp. 1183–1188, 2011.

[41] A. Ishak, "Similarity solutions for flow and heat transfer over a permeable surface with convective boundary condition," *Applied Mathematics and Computation*, vol. 217, no. 2, pp. 837–842, 2010.

[42] T. Hayat, Z. Iqbal, M. Mustafa, and S. Obaidat, "Boundary layer flow of an Oldroyd-B fluid with convective boundary conditions," *Heat Transfer: Asian Research*, vol. 40, no. 8, pp. 744–755, 2011.

[43] A. Alsaedi, M. Awais, and T. Hayat, "Effects of heat generation/absorption on stagnation point flow of nanofluid over a surface with convective boundary conditions," *Communications in Nonlinear Science and Numerical Simulation*, vol. 17, no. 11, pp. 4210–4223, 2012.

[44] M. Khan, R. Ali, and A. Shahzad, "MHD Falkner-Skan flow with mixed convection and convective boundary conditions," *Walailak Journal of Science and Technology*, vol. 10, no. 5, pp. 517–529, 2013.

[45] C. Y. Wang, "Analysis of viscous flow due to a stretching sheet with surface slip and suction," *Nonlinear Analysis: Real World Applications*, vol. 10, no. 1, pp. 375–380, 2009.

[46] T. Fang, J. Zhang, and S. Yao, "Slip MHD viscous flow over a stretching sheet—an exact solution," *Communications in Nonlinear Science and Numerical Simulation*, vol. 14, no. 11, pp. 3731–3737, 2009.

[47] S. Mukhopadhyay and H. I. Andersson, "Effects of slip and heat transfer analysis of flow over an unsteady stretching surface," *Heat and Mass Transfer*, vol. 45, no. 11, pp. 1447–1452, 2009.

[48] K. Bhattacharyya, S. Mukhopadhyay, and G. C. Layek, "Slip effects on boundary layer stagnation-point flow and heat transfer towards a shrinking sheet," *International Journal of Heat and Mass Transfer*, vol. 54, no. 1–3, pp. 308–313, 2011.

[49] F. Aman, A. Ishak, and I. Pop, "Mixed convection boundary layer flow near stagnation-point on vertical surface with slip," *Applied Mathematics and Mechanics. English Edition*, vol. 32, no. 12, pp. 1599–1606, 2011.

[50] T. Fang, S. Yao, J. Zhang, and A. Aziz, "Viscous flow over a shrinking sheet with a second order slip flow model," *Communications in Nonlinear Science and Numerical Simulation*, vol. 15, no. 7, pp. 1831–1842, 2010.

[51] L. P. Jentoft, Y. Tenzer, D. Vogt, J. Liu, R. J. Wood, and R. D. Howe, "Flexible, stretchable tactile arrays from MEMS barometers," in *Proceedings of the 16th International Conference on Advanced Robotics (ICAR '13)*, November 2013.

[52] M. Arunachalam and N. R. Rajappa, "Forced convection in liquid metals with variable thermal conductivity and capacity," *Acta Mechanica*, vol. 31, no. 1-2, pp. 25–31, 1978.

[53] T. C. Chiam, "Heat transfer in a fluid with variable thermal conductivity over a linearly stretching sheet," *Acta Mechanica*, vol. 129, no. 1-2, pp. 63–72, 1998.

[54] M. A. Seddeek and A. M. Salem, "Laminar mixed convection adjacent to vertical continuously stretching sheets with variable viscosity and variable thermal diffusivity," *Heat and Mass Transfer/Waerme- und Stoffuebertragung*, vol. 41, no. 12, pp. 1048–1055, 2005.

[55] J. Maxwell, *A Treatise on Electricity and Magnetism*, Oxford University Press, Cambridge, UK, 2nd edition, 1904.

[56] H. C. Brinkman, "The viscosity of concentrated suspensions and solutions," *The Journal of Chemical Physics*, vol. 20, pp. 571–581, 1952.

[57] V. R. Prasad, N. B. Reddy, R. Muthucumaraswamy, and B. Vasu, "Finite difference analysis of radiative free convection flow past an impulsively started vertical plate with variable heat and mass flux," *Journal of Applied Fluid Mechanics*, vol. 4, no. 1, pp. 59–68, 2011.